Caspase-independent cell engulfment mirrors cell death pattern in *Drosophila* embryos

Jaime Mergliano and Jonathan S. Minden*

Department of Biological Sciences and Science and Technology Center for Light Microscope Imaging and Biotechnology, Carnegie Mellon University, 4400 Fifth Avenue, Pittsburgh, PA 15213, USA
*Author of correspondence (e-mail: minden@cmu.edu)

Accepted 20 August 2003

Development 130, 5779-5789
© 2003 The Company of Biologists Ltd
doi:10.1242/dev.00824

Summary

Programmed cell death plays an essential role during *Drosophila* embryonic development. A stereotypic series of cellular changes occur during apoptosis, most of which are initiated by a caspase cascade that is triggered by a trio of proteins, RPR, HID and GRIM. The final step in apoptosis is engulfment of the cell corpse. To monitor cell engulfment in vivo, we developed a fluorogenic β-galactosidase substrate that is cleaved by an endogenous, lysosomal β-galactosidase activity. The pattern of cell engulfment in wild-type embryos correlated well with the known pattern of apoptosis. Surprisingly, the pattern of cell engulfment persisted in apoptosis-deficient embryos. We provide evidence for a caspase-independent engulfment process that affects the majority of cells expected to die in developing *Drosophila* embryos.

Key words: *Drosophila*, Embryo, Engulfment, Apoptosis, H99, p35, Phagocytosis

Introduction

The purpose of apoptosis is to orchestrate the orderly removal of cells from a tissue without spilling their contents into the intracellular space. In embryonic development, this process is essential for pattern formation, tissue homeostasis and the repair of patterning defects (Namba et al., 1997) (reviewed by Richardson and Kumar, 2002). The removal of cell corpses is also required to maintain cell signaling during pattern formation and for tissue morphogenesis (Li et al., 1999; Franc, 2002). Apoptosis follows a stereotypic sequence of cellular events. First, the dying cell pulls away from its neighbors, the nucleus becomes pyknotic and then fragments along with the chromosomes, the plasma membrane blebs and finally the cell is engulfed. There are a number of well-studied molecular pathways that underlie these cellular events. The most common scenarios involve a variety of cell signaling events that trigger mitochondrial changes which lead to the release of cytochrome *c* into the cytoplasm. This leads to the activation of a caspase cascade that results in the systematic degradation of a number of key proteins which drive the gross cellular changes and ultimately lead to the engulfment of the dying cell (Abrams, 1999; Lee and Baehrecke, 2000; Richardson and Kumar, 2002). These mechanisms are highly conserved from *C. elegans* to *Drosophila* to mammals.

A number of *Drosophila* genes necessary for cell death have been identified (Abrams, 1999; Lee and Baehrecke, 2000; Richardson and Kumar, 2002). *Drosophila* cells carry a full complement of caspases that are maintained in an inactive state by *Drosophila* inhibitor of apoptosis 1, DIAP1 (Hay, 2000). A trio of well-characterized cell death genes are known to inhibit DIAP1 and allow for caspase activation and cell death (White et al., 1994). These genes, *reaper* (*rpr*), *head involution defective* (*hid*) and *grim* lie in close proximity to one another on the third chromosome in a region spanned by the *H99* deletion. Embryos that are homozygous for the *H99* deletion lack cell death and exhibit several developmental abnormalities, including hyperplasia of the central nervous system, defects in head involution and delayed germband retraction (White et al., 1994; Pazdera et al., 1998; Vucic et al., 1998; Wang et al., 1999; Goyal et al., 2000; Holley et al., 2002; Yoo et al., 2002). Ectopic expression of these genes, alone or in combination, causes apoptosis in a tissue dependent fashion (Chen et al., 1998; Quinn et al., 2000).

Several other regulators of cell death are known in *Drosophila* that also have homologues in *C. elegans* and mammalian cells. DARK, which is homologous to CED-4 and APAF-1 in *C. elegans* and mammalian cells, respectively, is an apoptosis adaptor protein that functions downstream of RPR, HID and GRIM (Rodriguez et al., 1999). DARK initiates caspase function by binding to the class I caspases, DRONC and DREDD (Rodriguez et al., 1999; Kanuka et al., 1999). *dark* mutant embryos show reduced levels of cell death and hyperplasia in the central nervous system (Rodriguez et al., 1999; Kanuka et al., 1999). *debcl*, the *Drosophila* homologue of *ced-9* and a member of the *Bcl2/Bax* family, causes increased apoptosis when overexpressed and reduced cell death when inhibited by RNA interference (Colussi et al., 2000; Igaki et al., 2000; Zhang et al., 2000; Chen and Abrams, 2000).

One of the most challenging aspects of studying apoptosis is developing assays to measure the various cellular events that occur during cell death. The majority of our knowledge about apoptosis is derived from genetic analysis of *C. elegans* and from mammalian tissue culture systems. Time-lapse analysis of *C. elegans* mutants has uncovered a long list of genes required for cell death and phagocytosis. This time-lapse analysis relies on transmitted light microscopy to observe

cellular changes. Tissue culture systems have revealed many of the biochemical details about the signals leading to caspase activation and the caspase activation cascade itself. In addition, the tissue culture methods use transmitted-light microscopy and assays for nuclear decay, such as TUNEL and Acridine Orange (AO) staining. A very useful marker for plasma membrane changes during apoptosis is the flipping of phosphatidylserine from the inner leaflet to the outer surface of the membrane (Martin et al., 1995). Unfortunately, most of these methods are not suitable for studying apoptosis in living insects or mammals.

Cell death is a highly dynamic and patterned process. To monitor cell death in living *Drosophila* embryos, we have used time-lapse microscopy of AO-injected embryos (Pazdera et al., 1998). This revealed that apoptosis in the abdominal epidermis is patterned with a majority of cells dying adjacent to the segment boundaries. Removal of apoptotic cells by macrophages and neighboring cells occurs in approximately 40 minutes of the first appearance of an AO signal.

In *C. elegans*, the pattern of cell death is invariant. In organisms that employ regulative development, such as *Drosophila* and mammals, cell death is a more stochastic process. In these organisms, most tissues are formed from an excess of cells. Apoptosis is required to remove these excess cells after pattern formation. Thus, it is likely that there will be additional factors involved in cell death in regulative organisms. One obvious distinction is that in *C. elegans* dying cells are engulfed by their immediate neighbors; whereas in *Drosophila* and mammals, apoptotic cells are engulfed by macrophages, as well as their neighbors. Thus, there are probably different engulfment signals.

Genetic analysis of cell death in *C. elegans* has revealed seven genes that are required for cell engulfment (Ellis et al., 1991). These seven genes can be grouped into two pathways: *ced-1*, *ced-6*, *ced-7* and *ced-2*, *ced-5*, *ced-10*, *ced-12* (Ellis et al., 1991; Gumienny et al., 2001). Six of these genes are required exclusively in the engulfing cells. Only *ced-7*, which is homologous to human *ABC1* (*ABCA1* – Human Gene Nomenclature Database) is required in both the dying cells and the engulfing cells. There are no known genes required for engulfment of a dying cell that are exclusively expressed in the dying cell.

Very little is known about engulfment in *Drosophila*. *Drosophila* homologues of the *C. elegans* engulfment genes have been identified: *draper* ≈ *ced-1*, *dcrk* ≈ *ced-2*, *myoblast city* ≈ *ced-5* (Wu and Horvitz, 1998; Nolan et al., 1998) and *rac1* ≈ *ced-10* (Galletta et al., 1999; Reddien and Horvitz, 2000; Hakeda-Suzuki et al., 2002). Because an in vivo assay for phagocytosis in *Drosophila* embryos has not been established, the role of these genes in cell engulfment is not known. *croquemort* (*crq*), which is homologous to mammalian *CD36*, encodes a macrophage receptor for dying cells (Franc et al., 1996; Franc et al., 1999). Ectopic expression of *crq* is sufficient to confer phagocytic ability on non-phagocytic cells (Franc et al., 1996). The ligand for *crq* has not been identified.

To begin investigating phagocytosis in living *Drosophila* embryos, we developed a novel engulfment assay based on a fluorogenic β-galactosidase substrate, which we call VGAL. VGAL is non-fluorescent in the cytoplasm of living cells, but becomes fluorescent when a cell is phagocytosed by a neighbor or macrophage. The pattern of engulfment closely paralleled the cell death pattern as indicated by Acridine Orange fluorescence. Thus, we have developed a reliable in vivo assay for studying phagocytosis in living embryos. Surprisingly, the pattern of cell engulfment persisted in embryos that were deficient for *hid*, *rpr*, and *grim*. Likewise, the engulfment pattern persisted in embryos that globally expressed the pan-caspase inhibitor, p35. These results indicate that there is a significant caspase-independent, cell engulfment pathway operating in *Drosophila* embryos.

Materials and methods

Fly stocks

The following fly stocks were used (the chromosomal location of the UAS transgenes are shown in brackets): *UAS-p35* [2], *UAS-GFP(S65T)*[3] (referred to as *UAS-cGFP*), *H99/TM3* and *UAS-GFPnls*^{14} [2] (referred to as *UAS-nGFP*), were obtained from the Bloomington Stock Center, and *UAS-rpr, UAS-hid/TM3* [3] (J. Nambu). *UAS-p35; UAS-cGFP* and *UAS-nGFP; H99/TM3* were created from the above stocks.

Embryo preparation

Embryos were collected at stage 3 and prepared for time-lapse imaging and photoactivation as previously described (Minden et al., 2000). Briefly, embryos were collected on apple juice agar plates, dechorionated in 50% bleach for 90 seconds, then rinsed in egg-wash solution (0.12 M NaCl and 0.04% Triton X-100). Selected embryos were aligned on an agar block, placed onto a glue-coated coverslip and oriented with watchmaker's forceps so that the region to be imaged or photoactivated was flush with the coverslip. Embryos were staged by morphology according to Campus-Ortega and Hartenstein (Campus-Ortega and Hartenstein, 1985).

Time-lapse microscopy

Time-lapse microscopy was performed using a Delta Vision microscope system controlled by softWoRx software (Applied Precision, Issaquah, WA) configured around an Olympus IX70 inverted microscope. Dying cells were visualized by injection of Acridine Orange (0.25-0.5 mg/ml) into syncytial embryos and imaged with a fluorescein filter set. Cellular engulfment was visualized by injection of an in vivo β-galactosidase substrate, resorufin-β-galactoside-polyethylene glycol$_{1,900}$ (referred to as VGAL), at 1.8 mg/ml and imaged with a rhodamine filter set (Minden, 1996). Segment boundaries were observed with transmitted light.

Photoactivated gene expression

Photoactivated gene expression was done as previously described (Cambridge et al., 1997; Minden et al., 2000). Briefly, GAL4VP16 protein was purified and caged with nitroveratryl chloroformate. Caged GAL4VP16, at 115 μg/ml, was injected into syncytial embryos. Photoactivation was performed on an IX70 Olympus microscope using a DAPI bandpass filter to generate a beam of 365 nm light. The beam diameter was adjusted using different sized pinholes inserted into the conjugate image plane on one side of a dual-beam, epi-fluorescence illuminator. After photoactivation, the embryos were imaged by time-lapse microscopy.

Results

VGAL, a novel engulfment marker

Apoptosis is a highly dynamic process. To monitor cell death in living embryos, we have developed a number of time-lapse methods. The most prominent feature of apoptosis is nuclear decay, which is detected by increased Acridine Orange (AO)

fluorescence (Darzynkiewicz and Kapuscinski, 1990). In live cells, AO, which is weakly basic, is sequestered in acidic compartments such as lysosomes and is prevented from entering the nucleus (Clerc and Barenholz, 1998). When a cell receives a death signal, mitochondria cease to function, causing the pH gradient across the lysosomes to be lost. AO is released into the cytoplasm where it is able to enter the nucleus, bind to partially uncoiled DNA and become highly fluorescent (Delic et al., 1991). The dying cells, with their AO-positive nuclei, are subsequently engulfed by macrophages or neighboring cells, resulting in the secondary labeling of macrophages and neighboring cells with AO-positive vacuoles.

The final step in apoptosis is the engulfment of the cell corpse. Although there is a great deal known about apoptotic cell engulfment in *C. elegans*, there is very little known about this process in *Drosophila*. Our goal was to establish an in vivo engulfment assay using a fluorogenic, membrane-impermeant β-galactosidase substrate, resorufin-β-galactoside-polyethylene glycol$_{1,900}$ (referred to as VGAL) (Minden, 1996). Two key features of VGAL are: the β-galactoside-quenched resorufin fluorophore, which develops a red fluorescence when cleaved by β-galactosidase, and the long hydrophilic, polyethylene glycol tail that prevents the compound from crossing lipid membranes or gap junctions. *Drosophila* embryos have an endogenous, lysosomal β-galactosidase activity (MacIntyre, 1974; Fuerst et al., 1987). Injecting VGAL into the cytoplasm of syncytial-stage embryos loads it into all cells of the embryo where it is maintained in a non-fluorescent state. We reasoned that when a cell is engulfed, the cytoplasmic VGAL of the engulfed cell would be mixed with the β-galactosidase-containing, lysosomal compartment of the engulfing cell. This would lead to the cleavage of VGAL and cause the lysosomes of the engulfing cell to fluoresce red. To demonstrate this effect, syncytial-stage embryos were co-injected with AO and VGAL. Prior to the start of germband retraction, at late stage 11, there was no fluorescence from either fluorophore, aside from background yolk auto-fluorescence. Cell death first appears after the start of germband retraction as evidenced by the green fluorescence of AO-positive nuclei in the head and abdominal epidermis. Soon after the first AO-positive nuclei appear, the dying cells are engulfed by migrating macrophages. This is particularly evident in the head and tip of the retracting germband. After a lag of about 15 minutes, one can see red fluorescent bodies within the migrating macrophages (Fig. 1A-C). These VGAL-positive bodies ranged in size from 1-3 μm. The AO-positive and VGAL-positive vacuoles were mostly non-overlapping, indicating that the macrophages engulf cells in a piecemeal fashion. This has been observed in time-lapse recordings where several macrophages appeared to participate in engulfing a single dying cell (data not shown).

As VGAL is an unconventional marker for lysosomal activity, we compared the VGAL signal to a known fluorogenic lysosomal marker, DQ Red BSA (Molecular Probes). DQ Red BSA is a highly-labeled derivative of BSA, so much so that the fluorophores self-quench (Voss et al., 1996). When DQ Red BSA is cleaved by proteolysis, the fluorophores are free to diffuse apart and become fluorescent. Syncytial embryos that were co-injected with AO and DQ Red BSA displayed the same fluorescent labeling pattern of macrophages as did AO- and VGAL-injected embryos (Fig. 1D-F). The fluorescence intensity of cleaved DQ Red BSA was significantly less than the VGAL signal. In our hands, DQ Red BSA was quite variable and one had to use relatively high concentrations of this reagent to obtain a detectable signal. Thus, VGAL proved to be a sensitive engulfment marker.

To demonstrate that the large, motile cells that contained the AO- and VGAL-positive vacuoles were indeed macrophages, we used the photoactivated gene expression system (Cambridge et al., 1997) to activate *UAS-nGFP* expression selectively in macrophage progenitors. The photoactivated gene expression system relies on the injection of a caged form of the transcriptional activator, GAL4VP16 into syncytial embryos. Expression of a UAS-transgene is activated by briefly irradiating the cells of interest with a long-wavelength, UV microbeam, causing the uncaging of the GAL4VP16 protein.

Macrophages originate from a small patch of ventral mesoderm cells just anterior to the cephalic furrow (Tepass et al., 1994). Syncytial *UAS-nGFP* embryos were co-injected with caged-GAL4VP16 and VGAL and a patch of five to eight cells in this region was photoactivated at the start of gastrulation, causing them to express nuclear-localized GFP. The resulting nGFP-positive macrophages migrated throughout the embryo along their characteristic pathways. Some of these marked macrophages contained two GFP bodies (Fig. 1G). One of these is mostly likely the functional nucleus, while the other object is an engulfed nucleus derived from another photoactivated cell. The size of the photoactivation beam did not limit the irradiated area to macrophage precursors only. Over time, these marked macrophages accumulated red-fluorescent, VGAL-positive vacuoles. All photoactivated embryos with nGFP-positive macrophages contained VGAL-positive vacuoles of the same size range as observed in the AO-VGAL-injected embryos (9/9 embryos, Fig. 1G-I).

To demonstrate that dying cells elicit both AO and VGAL responses, the photoactivated gene expression system was used to induce a patch of apoptotic cells. *UAS-rpr, UAS-hid/TM3* embryos were co-injected with caged GAL4VP16, AO and VGAL. A patch of five to eight cells in the abdominal epidermis was photoactivated at the start of gastrulation (4 hours prior to the first apoptotic events) and analyzed by time-lapse microscopy (Fig. 1J-O). The first AO-positive, ectopic cell deaths appeared near the end of full germband elongation just prior to the start of germband retraction (Fig. 1J). Normally, endogenous cell death begins at the start of germband retraction. Ectopic VGAL-positive vacuoles were observed within 15 minutes of the AO-positive nuclei (8/8 embryos containing ectopic AO-positive nuclei, Fig. 1K). This time-lapse series shows a number of AO- and VGAL-positive spots persisting over the following 80 minutes (Fig. 1L-O). The duration of the AO signal was longer in these experiments than previously reported because the experiments were performed at 18°C, rather than 22°C, which slows development by about half. This characterization of VGAL indicates that it is a reliable and sensitive in vivo marker for apoptotic cell engulfment.

In vivo mapping of engulfment in wild-type embryos

Previous studies showed that cell death in the abdominal epidermis is patterned (Pazdera et al., 1998). Cell death begins at late stage 11, during the initiation of germband retraction, and continues through development to hatching. Time-lapse

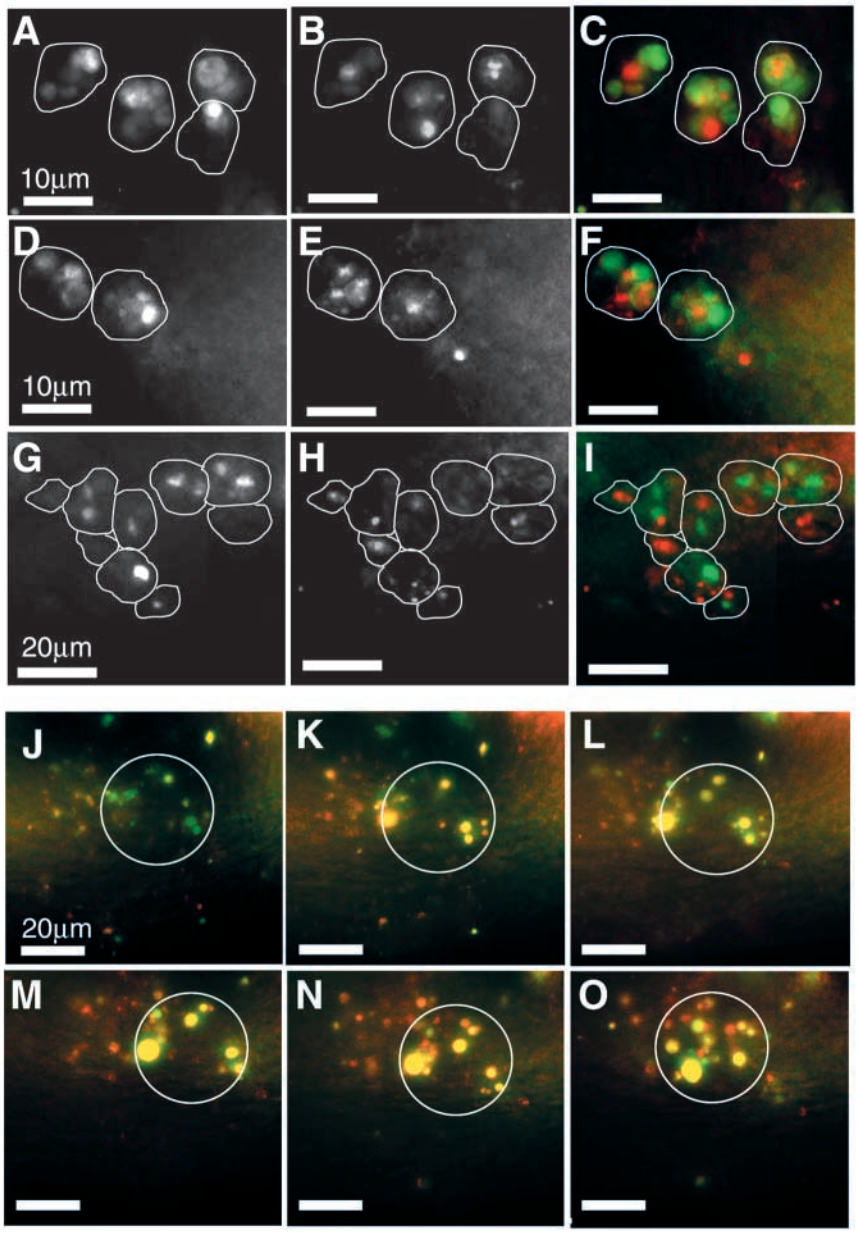

Fig. 1. Engulfment assay using VGAL. (A-C) A syncytial-blastoderm wild-type embryo was injected with AO and VGAL and a three-dimensional, time-lapse recording was made. Shown here is a single optical section of one time point at stage 14/15 of the AO, green fluorescence (A), VGAL, red fluorescence (B) and a composite image of both fluorescent channels (C). (A-I) The engulfing macrophages are outlined with a white line. (D-F) A syncytial-blastoderm wild-type embryo was injected with AO and DQ Red BSA and a three-dimensional, time-lapse recording was made. Shown here is a projection of two 4 μm optical sections of a single time point at stage 14/15 of the AO, green fluorescence (D), DQ Red BSA, red fluorescence (E) and a composite image of both fluorescent channels (F). (G-I) A *UAS-nGFP* embryo was injected with caged GAL4VP16 and VGAL and a five- to eight-cell patch of cells in the ventral furrow just anterior to the cephalic furrow was photoactivated. Shown here is a projection of two 5 μm optical sections of a single time point of a stage 14/15 embryo of the GFP fluorescence (G), VGAL fluorescence (H) and a composite of both fluorescent channels (I). (J-O) A *UAS-rpr; UAS-hid* embryo was injected with caged GAL4VP16, AO and VGAL and a five- to eight-cell patch of cells was photoactivated in the lateral epidermis. Shown here is a series of images that are projections of three 4 μm optical sections from a time-lapse recording at 20 minute intervals from the first appearance of the AO-positive ectopic cell death. The AO signal is shown as green and the VGAL signal as red. The photoactivated region is indicated by the white circle. Notice that the position of the circle changed over time as the embryo developed. Some of the VGAL-positive spots within 10 μm of the circle originated from the photoactivated region, further VGAL-spots are from naturally dying cells outside the photoactivated zone.

recordings of AO-injected embryos revealed that cell death occurs adjacent to the segment boundaries in three clusters along the dorsoventral axis. These initial studies also showed that dying epidermal cells in the abdomen are preferentially engulfed by their epithelial neighbors, not macrophages.

To explore the relationship between dying cells and their engulfment, we used time-lapse microscopy of embryos injected with AO and VGAL to map cell death and engulfment in the lateral abdominal epidermis. As was the case with macrophages, AO-positive nuclei generally appeared in the abdominal epidermis slightly before VGAL-positive vacuoles, with a lag of about 15 minutes. In addition, like the macrophages, the VGAL spots did not exactly overlap with the AO spots. However, the overall segmentally repeated, striped distribution of AO- and VGAL-spots was very similar. Fig. 2 shows selected images from a time-lapse recording of a wild-type embryo injected with AO and VGAL at 1/2, 3/4 and full germband retraction. These results confirm that dead epidermal cells are engulfed by their neighbors and that the VGAL pattern of engulfment mimics the AO pattern of apoptosis.

It is a formal possibility that the VGAL-positive spots in the epidermis could have arisen by a mechanism unrelated to cell death. To determine if there is a spatial and temporal correlation between the appearance of AO-positive nuclei of dying cells and VGAL-spots, we measured the distance between these objects with respect to when they first appeared. Imagine a scenario where a dying cell is engulfed by two flanking cells. If one flanking cell engulfed the nucleus of the dying cell while the other engulfed some of the cytoplasm of the dying cell's, one would expect the furthest separation between the AO-stained nucleus and the VGAL-stained lysosome to be less than two cell diameters apart, which would be 10-12 μm. Alternatively, if the VGAL signal was unrelated to the engulfment of a dying cell, one would expect the distance between an AO spot and VGAL spot to be quite variable. In addition, if the AO and VGAL signals are linked, the temporal

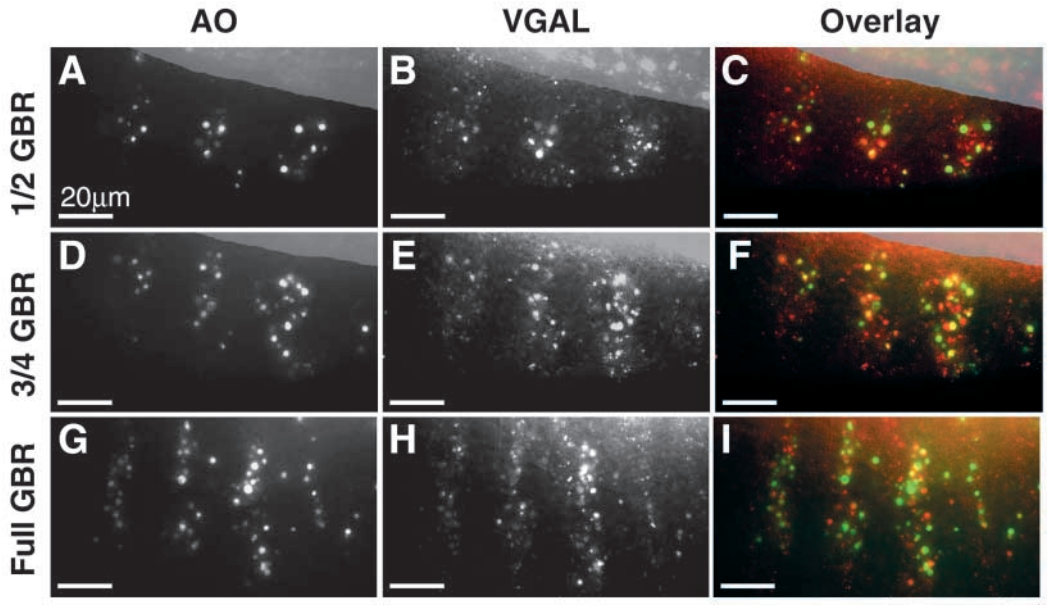

Fig. 2. Coincidence of AO and VGAL signals in the epidermis. A wild-type embryo was injected with AO and VGAL. (A-I) A series of images that are projections of five 2 μm optical sections from a time-lapse recording of the lateral epidermis. The embryo is shown at (A-C) 1/2 germband retraction (GBR), 3/4 GBR (D-F) and full GBR (G-I). (A,D,G) AO fluorescence; (B,E,H) VGAL fluorescence; (C,F,I) both fluorescence channels. A gray mask was applied to cover the amnioserosa.

separation between first appearances of these two signals will be less than 20 minutes. To test these hypotheses, we examined time-lapse recordings of wild-type embryos injected with AO and VGAL. The measurements were made as follows: VGAL spots along the lateral abdominal epidermis were chosen in random locations were cell death was just beginning. The VGAL spots were followed for 30 minutes and the closest AO spot was identified. The AO spot was then traced backwards in time to determine when it first appeared relative to its paired VGAL spot. Thus, we determined the nearest distance between pairs of AO and VGAL spots and the temporal separation between their initial appearances. This analysis was performed for 40 VGAL spots from a total of 11 segments in two embryos. All but one of these VGAL spots were within 10 μm of the closest AO-positive nucleus. Moreover, 33/40 were within 6 μm of the closest AO-positive nucleus, which is just over one cell diameter (Fig. 3J). In over half of cases, 23/40 the appearance of the AO-spot preceded that of the VGAL spot with an average time separation of 10 minutes. Six pairs appeared simultaneously; while the VGAL spots appeared prior to their AO partner in 10/40 pairs, with an average time separation of 7 minutes. We very rarely observed an AO-positive nucleus without a nearby VGAL-positive spot; conversely, VGAL-positive spots were rarely observed without a neighboring AO-positive nucleus. These data indicate that there is a significant spatial and temporal link between the appearance of VGAL and AO spots.

Previous time-lapse analysis of AO-injected embryos revealed a segmentally repeated pattern of cell death in the abdominal epidermis (Pazdera et al., 1998). To test the correlation between the patterns of VGAL-positive engulfment and the AO-positive cell death, the segmental distribution of VGAL spots was compared with that of AO spots. Time-lapse recordings of wild-type embryos injected only with VGAL were performed. Under acidic conditions, AO forms aggregates that weakly fluoresce red (Clerc and Barenholz, 1998). We have observed this weak, red fluorescence for AO, but it is much less intense than the VGAL signal. However, to be absolutely certain, AO was not co-injected to eliminate the possibility of any red fluorescence resulting from AO aggregates. The pattern of VGAL fluorescence when injected alone was very similar to that of VGAL plus AO (compare Fig. 3A-C with Fig. 2B,E,H, respectively). The distribution of VGAL spots across abdominal segments was determined by counting the number of VGAL spots within 12 μm of the embryo surface of 23 segments in a total of six VGAL-injected embryos at full germband retraction. Each segment was divided into three equal regions: anterior, middle and posterior. Slightly more than half of the VGAL spots occurred in the anterior third of each segment, with 29% found in the posterior third and only 20% of the VGAL spots appeared in the middle region of each segment (Fig. 3K). Thus, 80% of the VGAL spots were found at the segment boundaries. This is in close agreement with the distribution of AO spots in wild-type embryos (Pazdera et al., 1998). The VGAL spot distribution was not as pronounced as the AO distribution because we are counting VGAL spots after engulfment, which spreads the remains of dying cells into their neighbors. The AO distribution was determined by mapping the position of cell deaths when they first appeared, prior to engulfment.

The median number of VGAL spots per segment was 35±11. This is more than twice the number of dying cells, which is 12-16 cells per segment between stage 12-14 (Pazdera et al., 1998). Following the fate of AO-positive nuclei showed that 72% were fragmented into 2-7 pieces. This further demonstrates that dying cells are engulfed in multiple pieces.

Cell engulfment persists in cell-death-deficient embryos

To explore the relationship between AO-positive cell death and engulfment, we examined VGAL signaling in cell-death-deficient embryos. In *Drosophila*, apoptosis is controlled by a set of three closely linked genes: *hid*, *rpr* and *grim* (White et al., 1994). Embryos that are homozygous deficient for these three genes, which is covered by the *H99* deficiency, have very few AO-positive nuclei or engulfing macrophages (White et al., 1994). Preliminary experiments showed that homozygous *H99* embryos, that lacked AO-positive nuclei and macrophages,

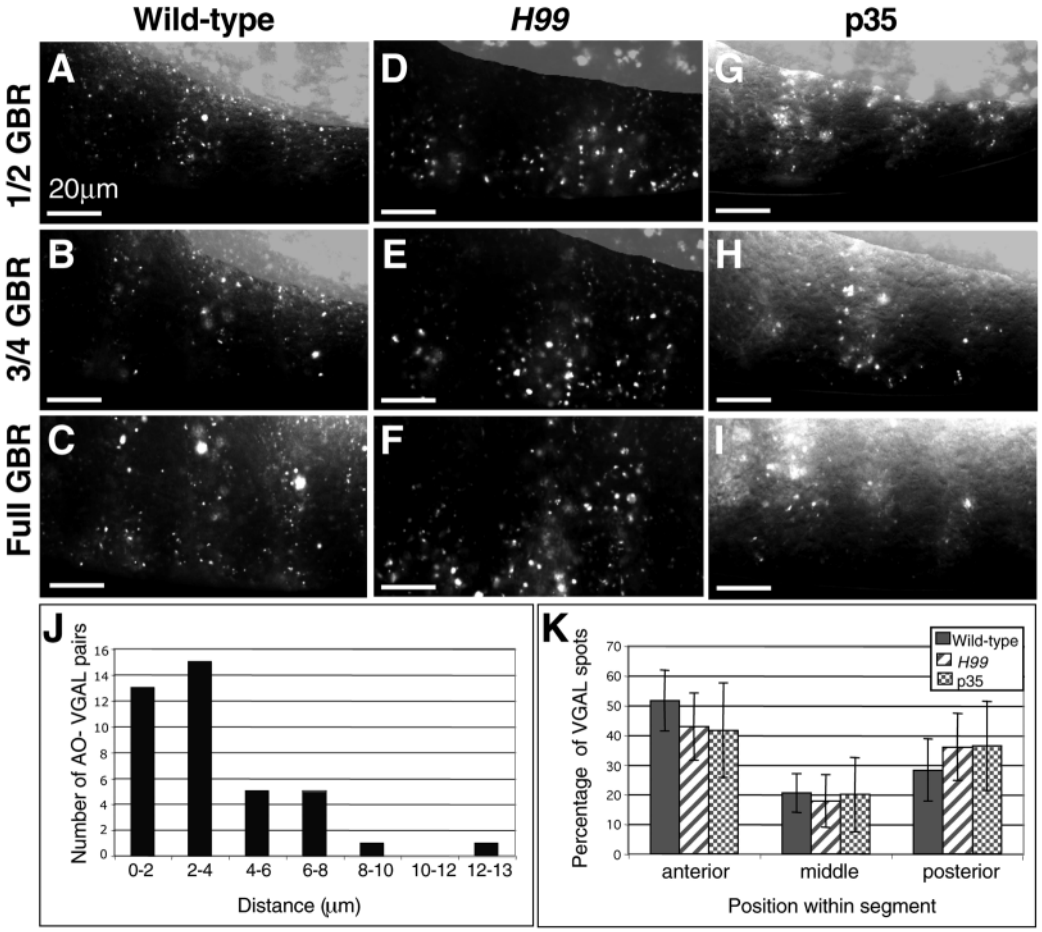

Fig. 3. Epidermal engulfment in the absence of cell death in *H99* and p35-expressing embryos. (A-F) A series of time-lapse images of (A-C) a wild-type embryo and (D-F) a homozygous *H99* embryo injected with VGAL: (A,D) 1/2 GBR, (B,E) 3/4 GBR and (C,F) full GBR. (G-I) A series of time-lapse images of a *UAS-p35; UAS-cGFP* embryo injected with caged GAL4VP16 and VGAL and exposed to whole-embryo photoactivation: (G) 1/2 GBR, (H) 3/4 GBR and (I) full GBR. The images in A-F are projections of four 3 μm optical sections; G-I are projections of three 3 μm optical sections. (J) Correlation between AO and VGAL signals. A histogram plotting the closest distance between VGAL and AO spots was measured within 30 minutes of the appearance of the VGAL signal, *n*=40 VGAL spots from 11 segments in two embryos. (K) Segmental distribution of VGAL spots within the lateral abdominal epidermis. A histogram showing the distribution of VGAL spots in the anterior, middle and posterior third of the abdominal segments in wild-type (solid bar), homozygous *H99* (hatched bar) and whole-embryo photoactivated *UAS-p35;UAS-cGFP* (checkered bar) embryos. The number of embryos samples was as follows. wild-type, *n*=23 segments from six embryos; homozygous *H99*, *n*=29 segments from five embryos; *UAS-P35;UAS-cGFP*, *n*=37 segments from 13 embryos.

also lacked VGAL-positive macrophages. Time-lapse recordings of *H99* embryos injected with VGAL alone were made. Embryos that lacked VGAL-positive macrophages were scored as homozygous for the *H99* deficiency, which accounted for the expected one quarter of all embryos examined. These embryos also displayed head involution and germband retraction defects. Surprisingly, all *H99* homozygous embryos developed the usual striped pattern of VGAL-positive spots in the epidermis (Fig. 3D-F). The temporal appearance of the VGAL signal was the same as wild-type embryos. There was no significant difference between the VGAL signal in wild-type and *H99* embryos with respect to the number or size of the VGAL spots.

To test if the engulfment pattern persisted in other cell-death-deficient paradigms, the photoactivated gene expression system was used to globally express the pan-caspase inhibitor, p35 (Hay et al., 1994). *UAS-p35* embryos were injected with caged GAL4VP16, AO and VGAL. Ninety percent of the irradiated embryos had fewer than 12 AO-positive nuclei per embryo, indicating that whole embryo irradiation globally activated p35 gene expression. To ensure that only segments expressing p35 were analyzed, *UAS-p35; UAS-cGFP* embryos were injected with caged GAL4VP16 and VGAL, then photoactivated over the entire embryo. The number of VGAL spots was counted in segments expressing GFP. All of these embryos continued to show segmentally repeated stripes of VGAL fluorescence (Fig. 3G-I). These photoactivated *UAS-p35* embryos had more VGAL-positive macrophages than did homozygous *H99* embryos, but the number of macrophages was significantly less than wild type. Most of these macrophages were restricted to the head region where the concentration of p35 was reduced due to limited diffusion of the caged GAL4VP16. Similar to homozygous *H99* embryos, global expression of p35 caused germband retraction defects in about half of the embryos.

Quantitation of the distribution and number of VGAL spots showed very similar values for wild-type, homozygous *H99* and p35-expressing embryos (the number for *H99* embryos was 29 segments in five embryos; the number for photoactivated *UAS-p35* embryos was 37 segments in 13 embryos). In all three cases, about 80% of the VGAL spots were located in the anterior or posterior third of the segment (Fig. 3K). Wild-type embryos appeared to have a bias toward the anterior compartment, while *H99* and p35-expressing embryos had a more even distribution that was still slightly biased to the anterior of the segment.

The average number of VGAL spots per segment was 30±10 in *H99* embryos. This was not significantly different from wild-

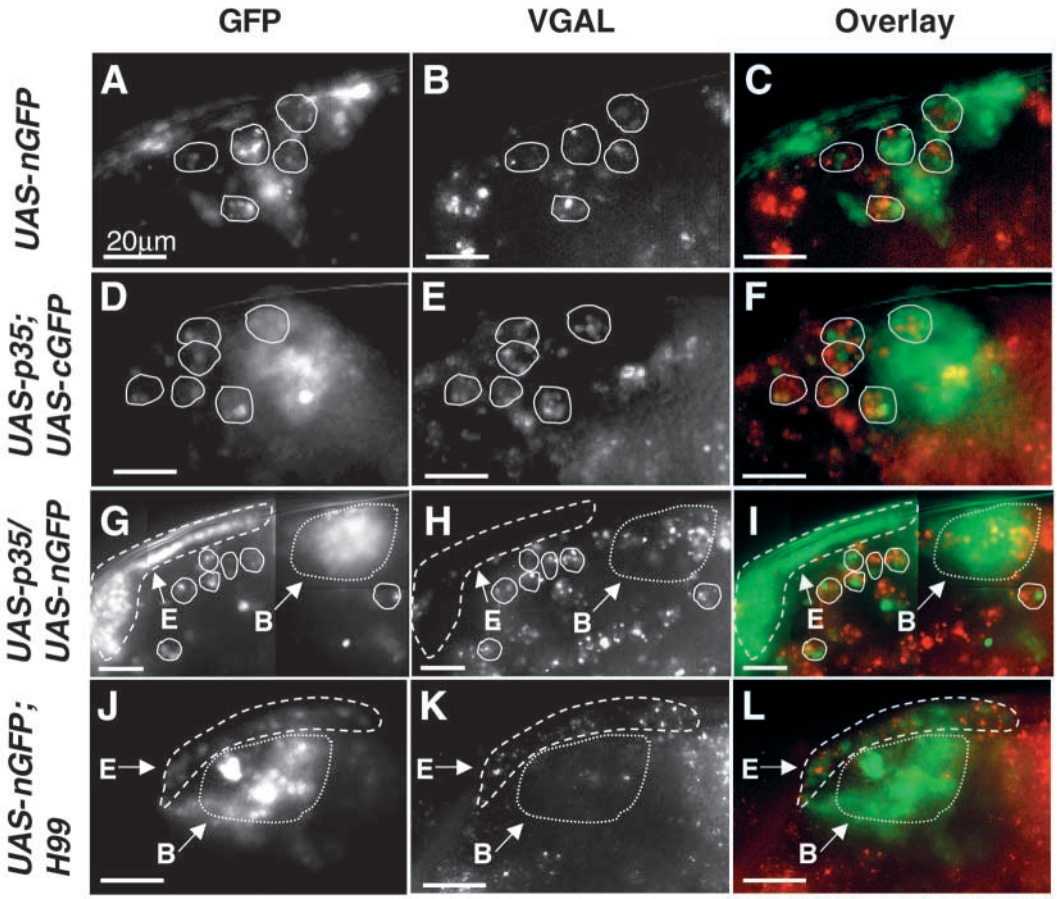

Fig. 4. Tissue-specific engulfment in wild-type, *H99* and p35-expressing cells. Brain neuronal precursors were marked by photoactivation of a *UAS-GFP* transgene in different genetic backgrounds. The embryos were injected with caged GAL4VP16 and VGAL, photoactivated in a five- to eight-cell patch of the head neuroectoderm and followed by time-lapse microscopy. The engulfing macrophages are outlined with a thin white line. (A-C) A projection of four 6 µm optical sections of a *UAS-nGFP* embryo with the GFP fluorescence (A), VGAL fluorescence (B) and a composite of both fluorescent channels (C). (D-F) A projection of three 5 µm optical sections of a *UAS-p35; UAS-cGFP* embryo with the GFP fluorescence (D), VGAL fluorescence (E) and a composite of both fluorescent channels (F). (G-I) A projection of eight 5 µm optical sections of a *UAS-p35/UAS-nGFP* embryo with the GFP fluorescence (G), VGAL fluorescence (H) and a composite of both fluorescent channels (I). In the GFP channel, the contrast of several regions was adjusted to equalize the fluorescence of marked epidermal and the brain cells to show their location. In G-L, epidermal cells are outlined with a dashed line and labeled 'E'; brain neurons are outlined with a dotted line and labeled 'B'. (J-L) A projection of four 5 µm optical sections of a *UAS-nGFP; H99* embryo with the GFP fluorescence (J), VGAL fluorescence (K) and a composite of both fluorescent channels (L).

type, which was 35±11. For p35-expressing embryos, the average was 18±6. This difference in spot number per segment can be attributed to the genetic background of the *UAS-p35* embryos, which had an average of 21±10 VGAL-positive spots per segment in the absence of p35 expression (35 segments in six embryos). These data indicate that the pattern of cell engulfment is unchanged in the absence of AO-positive cell death.

Engulfment of neuronal progenitors in *H99* and p35-expressing embryos

Inhibition of AO-positive cell death does not appear to affect the engulfment of cells expected to die in the epidermis. Dying epidermal cells are generally engulfed by neighboring cells. What is the fate of cells that are usually cleared by macrophage engulfment in caspase-inhibited embryos?

Dying neuronal cells are normally removed by macrophages. To demonstrate this, *UAS-nGFP* embryos were injected with caged GAL4VP16 and VGAL and a patch of five to eight cells was photoactivated in the lateral procephalic ectoderm of the early gastrula to mark neuronal progenitor and epidermal cells (Fig. 4A-C). The development and engulfment of GFP-positive cells was followed by time-lapse microscopy. Photoactivated cells that were engulfed gave rise to GFP-positive vacuoles within macrophages that also carried VGAL-positive vacuoles (*n*=14 embryos, Fig. 4A-C). This indicated the some of the cells emerging from the proneural region of the embryo had died and were engulfed by macrophages.

To test if inhibition of cell death by p35 altered macrophage engulfment, *UAS-p35; UAS-cGFP* embryos were injected with caged GAL4VP16 and VGAL. Notice that cytoplasmic GFP (cGFP) was used in this experiment instead of nuclear GFP. This was used to follow the fate of the cytoplasm of marked cells, not their nuclei; we suspected that the nuclei might not be engulfed. Photoactivating the same neurogenic region of the embryo gave rise to macrophages that harbored both VGAL- and GFP-containing vacuoles (*n*=9 embryos, Fig. 4D-F). These cells were identified as macrophages from time-lapse recordings because of their motile behavior. In addition, the GFP signal within these cells was confined to vacuoles that were the same size as the VGAL-containing vacuoles. This indicates that caspase-inhibited neuronal precursors continue to be engulfed by macrophages.

To determine if the entire cell, including the nucleus, was engulfed, *UAS-p35/UAS-nGFP* embryos were injected with caged GAL4VP16 and VGAL. As these embryos were heterozygous for *UAS-p35* and *UAS-nGFP*, the appropriate controls were performed to ensure that a sufficient amount of

p35 was induced to block AO-positive cell death and that a sufficient amount of nGFP was express to be visible (data not shown). Photoactivation of the neurogenic region generated GFP-positive brain neurons and over time gave rise to macrophages that harbored both VGAL- and GFP-containing vacuoles in all embryos examined (*n*=18, Fig. 4G-I). Thus, the presence of cGFP- and nGFP-vacuoles within macrophages indicates that caspase-inhibited cells are engulfed in entirety.

Homozygous *H99* embryos do not develop many engulfing macrophages. To determine the fate of neuronal precursors in homozygous *H99* embryos, *UAS-nGFP; H99/TM3* embryos were injected with caged GAL4VP16 and VGAL. The same population of neurogenic cells were photoactivated as stated above. Homozygous *H99* embryos were those that showed few VGAL-positive macrophages. Time-lapse recordings showed that dying epidermal progeny from this region of the embryo continued to be engulfed by neighbors, but the neuronal progeny were neither engulfed by macrophages nor by neighbors (*n*=7 embryos, Fig. 4J-L). Thus, localized, cell-autonomous caspase inhibition does not affect the engulfment of dying cells by macrophages, while globally blocking caspase activation appears to inhibit the phagocytic ability of macrophages.

Discussion

To establish an in vivo phagocytosis assay for *Drosophila* embryos, we employed a novel cell engulfment marker, VGAL, to map engulfment in the lateral epidermis in wild-type and cell death-deficient embryos. The following is a summary of the evidence for VGAL being a bonafide engulfment marker and for ruling out other possible mechanisms for eliciting VGAL fluorescence. VGAL is a membrane impermeant, fluorogenic β-galactosidase substrate. Biochemical and chemical studies have shown that VGAL is stable over a broad pH range and is specifically cleaved by β-galactosidase (Minden, 1996). The only known endogenous β-galactosidase activity in *Drosophila* is in lysosomes and the intervitelline space (MacIntyre, 1974; Fuerst et al., 1987; Minden, 1996). Injection of VGAL into the syncytial cytoplasm does not lead to VGAL fluorescence until late stage 11 when cell death and the engulfment of cell corpses first appears. The VGAL signal is confined to lysosome-size, subcellular vesicles that are 1-3 μm in diameter. The pattern of VGAL fluorescence was similar to a known lysosomal marker, DQ Red BSA; however, the QD Red BSA signal was neither as strong nor as reliable as the VGAL signal. There was no evidence of VGAL fluorescence filling the entire cytoplasmic space, which was seen when ectopic, cytoplasmic β-galactosidase was expressed by from *lacZ* transgenes (Minden, 1996). This demonstrates that the endogenous β-galactosidase is confined to the lysosome throughout development – it does not appear to leak out of the lysosomes even during cell death.

As VGAL is initially confined to the cytoplasm and there does not appear to be any cytoplasmic β-galactosidase activity, the only way to convert VGAL to its fluorescent form is to transport it into the lysosomal space. The usual routes into the lysosome are by engulfment or fluid-phase endocytosis. For endocytosis to occur, the VGAL must first leak out of the cell and then be taken up from the extracellular fluid. We do not believe this is happening for two reasons. First, we know that there is β-galactosidase activity in the intervitelline space. If VGAL was to leak out of cells into this space, one would observe an increase in intervitelline VGAL fluorescence, which was not seen. Second, if the VGAL was endocytosed from the extracellular fluid, one would expect to observe a broad distribution of VGAL, which was also not seen. The fact that the VGAL signal is distributed in a similar pattern both spatially and temporally as the AO-cell death pattern argues against a necrotic release of VGAL and subsequent endocytosis. One might argue that endocytosis of the released VGAL is so fast that there is little time for diffusion. If this were the case, one would not expect to observe VGAL in macrophages. The time it takes for a macrophage to migrate to a dying cell would be more than enough time for the released VGAL to be endocytosed by neighboring cells. The fact that macrophages carry VGAL-positive vesicles indicates engulfment of VGAL-containing cytoplasm.

We do not believe that secondary necrosis is contributing to the VGAL signal because secondary necrosis is primarily observed in tissue culture experiments where engulfment is not occurring and in vivo when massive amounts of apoptosis are induced and there are insufficient macrophages to clear the dying cells (Honda et al., 2000; Scaffidi et al., 2002). In the experiments reported here, we are mostly observing naturally occurring cell death. The appearance of the VGAL signal occurs within 10 minutes of the AO signal, thus there is not a significant delay in engulfment. Moreover, the timing of VGAL fluorescence is the same for both wild-type and *H99* embryos. Finally, intervitelline injection of the necrotic-cell marker, propidium iodide, did not label epidermal cells at any point during embryogenesis (J. Minden, personal communication).

The aforementioned arguments leave engulfment as the most likely cause for VGAL fluorescence. We cannot claim with certainty that the engulfment is solely by neighboring cells or macrophages and not by autophagy. Autophagy may play a role in eliciting a VGAL signal, but the distribution of the VGAL signal and the involvement of macrophages argues against significant amounts of autophagy. In autophagy, one would expect to see the VGAL signal to always appear immediately adjacent to apoptotic nuclei, which we do not generally observe. This evidence clearly indicates that VGAL is an authentic marker for cellular engulfment.

Surprisingly, engulfment occurred even in embryos known to be deficient for apoptotic cell death. Despite having no AO-positive cell death, homozygous *H99* embryos continued to show engulfment in the epidermis. The pattern and number of VGAL-positive vacuoles was the same as wild type. The VGAL-positive vacuoles were the same size in death-deficient embryos as in wild-type embryos. The persistence of the engulfment pattern in death-deficient embryos suggests that the cells expected to die in wild-type embryos are still experiencing the cellular changes required for their phagocytosis and still eliciting a signal for their neighbors to engulf them. The presence of phagocytosis in the absence of *rpr*, *hid* and *grim* suggests that there is a caspase-independent cell engulfment pathway and that the signal for engulfment occurs upstream of caspase activation. White et al. (White et al., 1994) observed a significant reduction of phagocytosis by macrophage in *H99* homozygous embryos using TEM analysis. We also observed the same reduction using time-lapse

microscopy. Thus, there may be two types of engulfment signal: a local signal for neighboring cells to phagocytose dying cells and a global signal that attracts macrophages to the site of cell death.

p35 is a pan-caspase inhibitor that functions by binding directly to caspases. This caspase inhibition is irreversible resulting from the cleavage of p35 (Bump et al., 1995; Zhou et al., 1998; LaCount et al., 2000). Previous studies have demonstrated that expression of p35 results in the loss of AO-positive cell death and leads to hyperplasia (Hay et al., 1994). As in death-deficient, homozygous *H99* embryos, p35-expressing embryos showed engulfment in a wild-type pattern in the lateral abdominal epidermis, in spite of not having any AO-positive nuclei. Furthermore, tissue specific expression of p35 in neuronal precursors showed that these marked cells were engulfed by macrophages that did not express p35. Thus, p35-expressing cells are capable of sending a global engulfment signal that attracts macrophages. It is curious that one does not observe many phagocytic macrophages in homozygous *H99* embryos. There are at least two possible explanations for this observation. (1) p35 does not inhibit all caspases, such as DRONC (Hawkins et al., 2000). DRONC is an initiator caspase that acts upstream of executioner caspases, which are p35 sensitive. One would expect that inhibiting the executioner caspases would inhibit all caspase-dependent cell death (Adrain and Martin, 2001). Perhaps these p35-resistant caspases are required for a dying cell to elicit a global engulfment signal. (2) A certain amount of cell death is required for macrophages to mature from non-phagocytic, hemocytes to mature, phagocytic macrophages (Tepass et al., 1994). Perhaps the signal from the cells being engulfed in death-deficient embryos is not sufficient to activate the macrophage population. Extensive DNA damage by X-irradiation of *H99* embryos indeed causes macrophages to engulf damaged cells (White et al., 1994), which is further evidence for a threshold for macrophage maturation. A third possible explanation, that was disproved, is that macrophages require caspase activation to be phagocytic. Photoactivating *UAS-p35* in macrophage precursors yielded macrophages that continued to be phagocytic (data not shown). Additional experimentation is required to determine why macrophages in homozygous *H99* embryos are not phagocytic.

One candidate for the local signal for cell engulfment is phosphatidylserine, which is flipped from the cytoplasmic face of the plasma membrane to the outer membrane surface of dying cells (Martin et al., 1995). The exposure of phosphatidylserine during death is a highly conserved process across multiple species from *C. elegans* to vertebrates (van den Eijnde et al., 1998). In addition, a phosphatidylserine receptor is found on virtually all cells capable of phagocytosis; activation of this receptor has been shown to lead to the engulfment of the dying cell (Fadok et al., 2001; Henson et al., 2001). We would very much like to monitor exposed phosphatidylserine in living *Drosophila* embryos. Unfortunately, this is not yet possible.

The results reported here indicate that the signal for cell engulfment may be independent of the caspase cascade. In addition to the vast literature on the necessity of caspases for apoptosis (Fraser and Evan, 1997; Fraser et al., 1997; Song et al., 1997; Chen et al., 1998; Dorstyn et al., 1999; Kumar and Doumanis, 2000; Quinn et al., 2000; Adrain and Martin, 2001; Harvey et al., 2001), there is growing evidence for caspase-independent death pathways in tissue culture paradigms (Borner and Monney, 1999; Leist and Jaattela, 2001; Lockshin and Zakeri, 2002). There are very few reports on caspase-independent cell death in vivo. In *Drosophila*, it has been shown that *rpr*, *hid* and *grim* are not required for apoptosis of the nurse cells during oogenesis (Foley and Cooley, 1998). Zhang et al. (Zhang et al., 2000) showed that Dbok is capable of inducing cytochrome *c* release in a caspase-independent fashion when overexpressed. These cultured *Drosophila* cells died in a non-apoptotic, presumably necrotic, fashion in the presence of zVAD-fmk, a broad range caspase inhibitor. It is very unlikely that the VGAL signal is the result of necrotic death for the reasons stated earlier.

A very important question about engulfment in cell-death-deficient embryos is why is there no AO signal from cells that have been engulfed? There are two possible explanations: (1) chromosomes within the lysosomes of engulfing cells do not adopt a suitable conformation for AO intercalation if they have not been previously exposed to caspase-activated endonucleases; or (2) the acidic environment of the lysosome maintains the AO in an aggregated state that is not amenable to DNA intercalation. Delic et al. (Delic et al., 1991) showed that chromosomes within living nuclei do not bind AO. A key feature of apoptosis is nuclear condensation. This condensation, which can be triggered by caspase activation, may be essential for AO binding. Further experimentation in vivo and in vitro is required to determine why engulfed cell nuclei do not elicit AO fluorescence in caspase-inhibited embryos.

If cell engulfed continues in caspase-inhibited embryos, then why do these embryos die? There is evidence that caspases are also required for morphogenesis. *rpr* is expressed in the embryo several hours before cell death appears in a pattern that covers many more cells than the number that actually die (Nassif et al., 1998; Pazdera et al., 1998). These observations spawned the notion that there is a threshold of *rpr* expression below which permits morphogenesis; above which triggers cell death. To further understand the relationship between morphogenesis and cell death, a detailed developmental analysis of embryos lacking various caspases alone or in combination must be performed.

Why do caspase-inhibited embryos have extra cells? White et al. (White et al., 1994) showed that there are extra cells in the CNS of homozygous *H99* embryos. Our time-lapse analysis has shown that dying neurons are generally cleared by macrophages. We and others have also shown that macrophages do not mature properly in homozygous *H99* embryos (Tepass et al., 1994). Therefore, the extra CNS cells in homozygous *H99* embryos may be due to an engulfment failure in addition to the blockage of the cell death program. We showed that localized inhibition of caspases by p35 does not block the expected phagocytosis of neuronal cells. In *C. elegans*, it has been shown that cells slated to die can be rescued in engulfment-deficient animals (Hoeppner et al., 2001; Reddien et al., 2001).

Finally, if cells are being engulfed in homozygous *H99* and global, p35-expressing embryos, should these still be considered cell-death-deficient embryos? Once a cell is engulfed, it should be considered dead. Therefore, homozygous *H99* and global, p35-expressing embryos should

not be referred to as cell-death-deficient; perhaps they should be referred to as caspase-inactivated or -inhibited embryos. It is not clear if this caspase-independent engulfment can still be considered apoptosis as the hallmark features of apoptosis do not occur in these embryos. One very important distinction must be made between the results reported here and much of the existing research on apoptosis. Aside from studies using *C. elegans* embryos, the vast majority of cell death research has focused on tissue culture models. In these tissue culture systems there are generally no engulfing cells present and it typically takes several hours for most cells to die upon triggering apoptosis. In living *Drosophila* embryos, AO-positive cells are engulfed within 15 minutes of the AO signal, and in some cases engulfment precedes the AO signal. The precise time lag between the decision for cell death and the AO- or VGAL-signals is not known. We estimate the lag to be about 1 hour. This is based on previous studies where excess cells resulting from an ectopic round of cell division driven by Cyclin E overexpression begin to produce ectopic AO signals within 1 hour of the ectopic division (Li et al., 1999). Thus, there are significant differences between cell death in situ and in culture. Exploring these differences will play an important role in our understanding of programmed cell death.

We thank Kara Coval for technical assistance, Chuck Ettensohn and the Minden laboratory for their critical reading of the manuscript, and John Nambu and the Bloomington Stock Center for fly stocks. This work was supported by a grant from the National Institutes of Health (HD031642) to J.S.M.

References

Abrams, J. (1999). An emerging blueprint for apoptosis in *Drosophila*. *Trends Cell Biol.* **9**, 435-440.

Adrain, C. and Martin, S. L. (2001). Search for *Drosophila* caspases bears fruit: STRICA enters the fray. *Cell Death Differ.* **8**, 319-323.

Borner, C. and Monney, L. (1999). Apoptosis without caspases: an inefficient molecular guillotine?, *Cell Death Differ.* **6**, 497-507.

Bump, N., Hackett, M., Hugunin, M., Seshagiri, S., Brady, K., Chen, P., Ferenz, C., Franklin, S., Ghayur, T., Li, P. et al. (1995). Inhibition of ICE family proteases by baculovirus antiapoptotic protein p35. *Science* **269**, 1185-1888.

Cambridge, S. B., Davis, R. and Minden, J. S. (1997). *Drosophila* mitotic domain boundaries as cell fate boundaries. *Science* **277**, 825-828.

Campus-Ortega, J. A. and Hartenstein, V. (1985). Stages of *Drosophila* embryogenesis. In *The Embryonic Development of* Drosophila melanogaster, pp. 9-84. Berlin: Springer-Verlag.

Chen, P. and Abrams, J. (2000). *Drosophila* apoptosis and Bcl-2 genes: outliers fly in. *J. Cell Biol.* **148**, 625-627.

Chen, P., Rodriguez, A., Erskine, R., Thach, T. and Abrams, J. M. (1998). Dredd, a novel effector of the apoptosis activators *reaper*, *grim*, and *hid* in *Drosophila*. *Dev. Biol.* **201**, 202-216.

Clerc, S. and Barenholz, Y. (1998). A quantitative model for using acridine orange as a transmembrane pH gradient probe. *Anal. Biochem.* **259**, 104-111.

Colussi, P., Quinn, L., Huang, D., Coombe, M., Read, S., Richardson, H. and Kumar, S. (2000). Debcl, a proapoptotic Bcl-2 homologue, is a component of the *Drosophila melanogaster* cell death machinery. *J. Cell Biol.* **148**, 703-714.

Darzynkiewicz, Z. and Kapuscinski, J. (1990). Acridine orange: A versitile probe of nucleic acids and other cell constituents. In *Flow Cytometry and Sorting*, 2nd edn (ed. M. R. Melamed, T. Lindmo and M. L. Mendelsohn), pp. 291-314. New York, NY: J. Wiley and Sons.

Delic, J., Coppey, J., Magdelenat, H. and Coppey-Moisan, M. (1991). Impossibility of acridine orange intercalation in nuclear DNA of the living cell. *Exp. Cell Res.* **194**, 147-153.

Dorstyn, L., Read, S., Quinn, L., Richardson, H. and Kumar, S. (1999). DECAY, a novel *Drosophila* caspase related to mammalian caspase-3 and caspase-7. *J. Biol. Chem.* **274**, 30778-30783.

Ellis, R., Jacobson, D. and Horvitz, H. (1991). Genes required for the engulfment of cell corpses during programmed cell death in *Caenorhabditis elegans*. *Genetics* **129**, 79-94.

Fadok, V., Xue, D. and Henson, P. (2001). If phosphatidylserine is the death knell, a new phosphatidylserine-specific receptor is the bellringer. *Cell Death Differ.* **8**, 582-587.

Foley, K. and Cooley, L. (1998). Apoptosis in late stage *Drosophila* nurse cells does not require genes within the *H99* deficiency. *Development* **125**, 1075-1082.

Franc, N. C. (2002). Phagocytosis of apoptotic cells in mammals, *Caenorhabditits elegans* and *Drosophila melanogaster*: Molecular mechanisms and physiological consequences. *Frontiers Biosci.* **7**, 1298-1313.

Franc, N., Dimarcq, J., Lagueux, M., Hoffman, J. and Ezekowitz, A. (1996). Croquemort, a novel *Drosophila* hemocyte/macrophage receptor that recognizes apoptotic cells. *Immunity* **4**, 431-443.

Franc, N., Heitzler, P., Ezekowitz, A. and White, K. (1999). Requirement for Croquemort in phagocytosis of apoptotic cells in *Drosophila*. *Science* **284**, 1991-1994.

Fraser, A. and Evan, G. (1997). Identification of a *Drosophila melanogaster* ICE/CED-3-related protease, drICE. *EMBO J.* **16**, 2805-2813.

Fraser, A., McCarthy, N. and Even, G. (1997). drICE is an essential caspase required for apoptotic activity in *Drosophila* cells. *EMBO J.* **16**, 6192-6199.

Fuerst, T. R., Knipple, D. C. and MacIntyre, R. J. (1987). Purification and characterization of beta-galactosidase-1 from *Drosophila* melanogaster. *Insect Biochem.* **17**, 1163-1171.

Galletta, B. J., Niu, X., Erickson, M. R. and Abmayr, S. M. (1999). Identification of a *Drosophila* homologue to vertebrate Crk by interaction with MBC. *Gene* **228**, 243-252.

Goyal, L., McCall, K., Agapite, J., Hartwieg, E. and Steller, H. (2000). Induction of apoptosis by *Drosophila reaper, hid*, and *grim* through inhibition of IAP function. *EMBO J.* **19**, 589-597.

Gumienny, T., Brugnera, E., Tosello-Trampont, A., Kinchen, J., Haney, L. B., Nishiwaki, K., Walk, S., Nemergut, M. E., Macara, I. G., Francis, R. et al. (2001). CED-12/ELMO, a novel member of the CrkII/Dock180/Rac pathway, is required for phagocytosis and cell migration. *Cell* **107**, 27-41.

Hakeda-Suzuki, S., Ng, J., Tzu, J., Dietzl, G., Sun, Y., Harms, M., Nardine, T., Luo, L. and Dickson, B. J. (2002). Rac function and regulation during *Drosophila* development. *Nature* **416**, 438-442.

Harvey, N., Daish, T., Mills, K., Dorstyn, L., Quinn, L., Read, S., Richardson, H. and Kumar, S. (2001). Characterization of the *Drosophila* caspase, DAMM. *J. Biol. Chem.* **276**, 25342-25350.

Hawkins, C. J., Yoo, S. J., Peterson, E. P., Wang, S. L., Vernooy, S. Y. and Hay, B. A. (2000). The *Drosophila* caspase DRONC cleaves following glutamate or aspartate and is regulated by DIAP1, HID, and GRIM. *J Biol. Chem.* **275**, 27084-27093.

Hay, B. (2000). Understanding IAP function and regulation: a view from *Drosophila*. *Cell Death Diff.* **7**, 1045-1056.

Hay, B., Wolff, T. and Rubin, G. (1994). Expression of baculovirus p35 prevents cell death in *Drosophila*. *Development*. **120**, 2121-2129.

Henson, P., Bratton, D. and Fadok, V. (2001). The phosphatidylserine receptor: a crucial molecular switch? *Nat. Rev. Mol. Cell Biol.* **2**, 627-633.

Hoeppner, D. J., Hengartner, M. O. and Schnabel, R. (2001). Engulfment genes cooperate with *ced-3* to promote cell death in *Ceanorhabditis elegans*. *Nature* **412**, 202-206.

Holley, C., Olson, M., Colon-Ramos, D. and Kornbluth, S. (2002). Reaper eliminates IAP proteins through stimulated IAP degradation and generalized translational inhibition. *Nat. Cell Biol.* **4**, 439-444.

Honda, O., Kuroda, M., Joja, I., Asaumi, J., Takeda, Y., Akaki, S., Togami, I., Kanazawa, S., Kawasaki, S. and Hiraki, Y. (2000). Assessment of secondary necrosis of Jurkat cells using a new microscopic system and double staining method with annexin V and propidium iodide. *Int. J. Oncol.* **16**, 283-288.

Igaki, T., Kanuka, H., Inohara, N., Sawamoto, K., Nunez, G., Okano, H. and Miura, M. (2000). Drob-1, a *Drosophila* member of the Bcl-2/CED-9 family that promotes cell death. *Proc. Natl. Acad. Sci. USA* **97**, 662-667.

Kanuka, H., Sawamoto, K., Inohara, N., Matsuno, K., Okano, H. and Miura, M. (1999). Control of the cell death pathway by Dapaf-1, a *Drosophila* Apaf-1/CED-4-related caspase activator. *Mol. Cell* **4**, 757-769.

Kumar, S. and Doumanis, J. (2000). The fly caspases. *Cell Death Differ.* **7**, 1039-1044.

LaCount, D., Hanson, S., Schneider, C. and Friesen, P. (2000). Caspase inhibitor p35 and inhibitor of apoptosis Op-IAP block *in vivo* proteolytic

activation of an effector caspase at different steps. *J. Biol. Chem.* **275**, 15657-15664.
Lee, C. Y. and Baehrecke, E. (2000). Genetic regulation of programmed cell death in *Drosophila*. *Cell Res.* **10**, 193-204.
Leist, M. and Jaattela, M. (2001). Four deaths and a funeral: from caspases to alternative mechanisms. *Nat. Rev. Mol. Cell Biol.* **2**, 589-598.
Li, Q. J., Pazdera, T. M. and Minden, J. S. (1999). *Drosophila* embryonic pattern repair: how embryos respond to cyclin E-induced ectopic cell division. *Development* **126**, 2299-2307.
Lockshin, R. A. and Zakeri, Z. (2002). Caspase-independent cell deaths. *Curr. Opin. Cell Biol.* **14**, 727-733.
MacIntyre, R. J. (1974). Preliminary genetic localization of several lysosomal gene-enzyme systems in *Drosophila melanogaster*. *Isozyme Bull.* **7**, 23-24.
Martin, S., Reutelingsperger, C., McGahon, A., Radar, J., van Schie, R., LaFace, D. and Green, D. (1995). Early redistribution of plasma membrane phosphatidylserine is a general feature of apoptosis regardless of the initiating stimulus: Inhibition by overexpression of Bcl-2 and Abl. *J. Exp. Med.* **182**, 1545-1556.
Minden, J. S. (1996). Synthesis of a new substrate for detection of *lacZ* gene expression in live *Drosophila* embryos. *BioTechniques* **20**, 122-129.
Minden, J. S., Namba, R., and Cambridge, S. (2000). Photoactivated gene expression for cell-fate mapping and cell manipulation. In Drosophila *Protocols* (ed. W. Sullivan, M. Ashburner and R. S. Hawley), pp 413-427. New York, NY: Cold Spring Harbor Laboratory Press.
Namba, R., Pazdera, T. M., Cerrone, R. L. and Minden, J. S. (1997). *Drosophila* embryonic pattern repair: how embryos respond to *bicoid* dosage alteration. *Development* **124**, 1393-1403.
Nassif, C., Daniel, A., Lengyel, J. A. and Hartenstein, V. (1998). The role of morphogenetic cell death during *Drosophila* embryonic head development. *Dev. Biol.* **197**, 170-186.
Nolan, K. M., Barrett, K., Lu, Y., Hu, K. Q., Mincent, S. and Settleman, J. (1998). Myoblast city, the *Drosophila* homolog of DOCK180/CED-5, is required in a Rac signaling pathway utilized for mulitple developmental processes. *Genes Dev.* **12**, 3337-3342.
Pazdera, T., Janaardhan, P. and Minden, J. S. (1998). Patterned epidermal cell death in wild-type and segment polarity mutant *Drosophila* embryos. *Development* **125**, 3427-3436.
Quinn, L., Dorstyn, L., Mills, K., Colussi, P., Chen, P., Coombe, M., Abrams, J., Kumar, S. and Richardson, H. (2000). An essential role for the caspase Dronc in developmentally programmed cell death in *Drosophila*. *J. Biol. Chem.* **275**, 40416-40424.
Reddien, P. W. and Horvitz, H. R. (2000). CED-2/CrkII and CED-10/Rac control phagocytosis and cell migration in *Caenorhabditits elegans*. *Nat. Cell Biol.* **2**, 131-136.
Reddien, P. W., Cameron, S. and Horvitz, H. R. (2001). Phagocytosis promotes programmed cell death in *C. elegans*. *Nature* **412**, 198-202.
Richardson, H. and Kumar, S. (2002). Death to flies: *Drosophila* as a model system to study programmed cell death. *J. Immunol. Meth.* **265**, 21-38.
Rodriguez, A., Oliver, H., Zou, H., Chen, P., Wang, X. and Abrams, J. (1999). Dark is a *Drosophila* homologue of Apaf-1/CED-4 and functions in an evolutionarily conserved pathway. *Nat. Cell Biol.* **1**, 272-279.
Scaffidi, P., Misteli, T. and Bianchi, M. E. (2002). Release of chromatin protein HMGB1 by necrotic cells triggers inflammation. *Science* **418**, 191-195.
Song, Z., McCall, K. and Steller, H. (1997). DCP-1, a *Drosophila* cell death protease essential for development. *Science* **275**, 536-540.
Tepass, U., Fessler, L. I., Aziz, A. and Hartenstein, V. (1994). Embryonic origin of hemocytes and their relationship to cell death in *Drosophila*. *Development* **120**, 1829-1837.
van den Eijnde, S., Boshart, L., Baehrecke, E., de Zeeuw, C., Reutelingsperger, C. and Vermeij-Keers, C. (1998). Cell surface exposure of phosphatidylserine during apoptosis is phylogenetically conserved. *Apoptosis* **3**, 9-16.
Voss, E. W., Workman, C. J. and Mummert, M. E. (1996). Detection of protease activity using a fluorescence-enhancement globular substrate. *Biotechniques* **20**, 286-291.
Vucic, D., Kaiser, W. and Miller, L. (1998). Inhibitor of apoptosis proteins physically interact with and block apoptosis induced by *Drosophila* proteins HID and GRIM. *Mol. Cell. Biol.* **18**, 3300-3309.
Wang, S., Hawkins, C., Yoo, S., Muller, H. and Hay, B. (1999). The *Drosophila* caspase inhibitor DIAP1 is essential for cell survival and is negatively regulated by HID. *Cell* **98**, 453-463.
White, K., Grether, M., Abrams, J., Young, L., Farrell, K. and Steller, H. (1994). Genetic control of programmed cell death in *Drosophila*. *Science* **264**, 677-682.
Wu, Y. C. and Horvitz, H. R. (1998). *C. elegans* phagocytosis and cell-migration protein CED-5 is similar to human DOCK180. *Nature* **329**, 501-504
Yoo, S., Huh, J., Muro, I., Wang, L., Wang, S., Feldman, R., Clen, R., Muller, H. and Hay, B. (2002). Hid, Rpr and Grim negatively regulate DIAP1 levels through distinct mechanisms. *Nat. Cell Biol.* **4**, 416-424.
Zhang, H., Huang, Q., Ke, N., Matsuyana, S., Hammock, B., Godzik, A. and Reed, J. (2000). *Drosophila* pro-apoptotic Bcl-2/Bax homologue reveals evolutionary conservation of cell death mechanisms. *J. Biol. Chem.* **275**, 27303-27306.
Zhou, Q., Krebs, J., Snipas, S., Price, A., Alnemri, E., Tomascelli, K. and Salvesen, G. (1998). Interaction of the baculovirus anti-apoptotic protein p35 with caspases. Specificity, kinetics, and characterization of the caspase/p35 complex. *Biochemistry* **37**, 10757-10765.